

2017-02-01

The cold climate geomorphology of the Eastern Cape Drakensberg: A reevaluation of past climatic conditions during the last glacial cycle in Southern Africa

Mills, SC

<http://hdl.handle.net/10026.1/8086>

10.1016/j.geomorph.2016.11.011

Geomorphology

Elsevier BV

All content in PEARL is protected by copyright law. Author manuscripts are made available in accordance with publisher policies. Please cite only the published version using the details provided on the item record or document. In the absence of an open licence (e.g. Creative Commons), permissions for further reuse of content should be sought from the publisher or author.

1 **The cold climate geomorphology of the Eastern Cape Drakensberg:**
2 **A reevaluation of past climatic conditions during the last glacial**
3 **cycle in southern Africa**

4
5 S. C. Mills^{1*}, T. T. Barrows², M. W. Telfer¹, L. K. Fifield³

6
7 ¹School of Geography, Earth and Environmental Sciences, Plymouth University,
8 Drake Circus, Plymouth, PL4 8AA, UK

9 ²Department of Geography, University of Exeter, Exeter, Devon EX4 4RJ, UK

10 ³Department of Nuclear Physics, Research School of Physics and Engineering,
11 Australian National University, Canberra, ACT 0200, Australia

12
13 *Corresponding author. Stephanie. C. Mills (stephanie.mills@plymouth.ac.uk)

14 Tel: (+44) (0)1752 585943.

15
16
17
18 **This manuscript is the final submitted version and contains errors that were**
19 **corrected during proofing. To access the published version, please see:**
20 <http://www.journals.elsevier.com/geomorphology>

21
22
23
24
25

26 **Abstract**

27 Southern Africa is located in a unique setting for investigating past cold climate
28 geomorphology over glacial-interglacial timescales. It lies at the junction of three of the
29 world's major oceans and is affected by subtropical and temperate circulation systems,
30 therefore recording changes in Southern Hemisphere circulation patterns. Cold
31 climate landforms are very sensitive to changes in climate and thus provide an
32 opportunity to investigate past changes in this region. The proposed existence of
33 glaciers in the high Eastern Cape Drakensberg mountains, together with possible rock
34 glaciers, has led to the suggestion that temperatures in this region were as much as
35 10-17°C lower than present. Such large temperature depressions are inconsistent with
36 many other palaeoclimatic proxies in southern Africa. This paper presents new field
37 observations and cosmogenic nuclide exposure ages from putative cold climate
38 landforms. We discuss alternative interpretations for the formation of the landforms
39 and confirm that glaciers were absent in the Eastern Cape Drakensberg during the
40 last glaciation. However, we find widespread evidence for periglacial activity down to
41 an elevation of ~1700 m asl, as illustrated by extensive solifluction deposits,
42 blockstreams, and stone garlands. These periglacial deposits suggest that the climate
43 was significantly colder (~6°C) during the Last Glacial Maximum, in keeping with other
44 climate proxy records from the region, but not cold enough to initiate or sustain glaciers
45 or rock glaciers.

46 *Keywords:* Eastern Cape Drakensberg; surface exposure dating; periglacial
47 geomorphology; palaeoclimate

48

49

50

51 **1. Introduction**

52 South Africa is positioned in a key location at the junction of three of the world's oceans
53 and experiences a range of different climatic regimes owing to the influence of global
54 circulation patterns and atmospheric processes. The magnitude of climate changes
55 that occur in this region over glacial-interglacial cycles remains controversial, and the
56 presence of glaciation in southern Africa during cold periods has attracted a wide
57 range of research over a number of decades (e.g., Sparrow, 1967; Sanger, 1988;
58 Marker, 1991; Grab, 1996, Lewis and Illgner, 2001; Mills and Grab, 2005; Mills et al.,
59 2009a,b, 2012; Hall, 2010). Glacial and periglacial landforms are highly sensitive to
60 temperature and precipitation and are excellent indicators of past climate change,
61 provided they are correctly identified. Lewis and Illgner (2001) and Lewis (2008a)
62 proposed that small glaciers could have existed at key sites in the high Eastern Cape
63 Drakensberg mountains as a result of topographic shading and snowblow. However,
64 the majority of recent work concerning past glaciation has been undertaken in Lesotho
65 (Fig. 1), where Mills et al. (2012) proposed the occurrence of small-scale glaciation at
66 much higher elevations. Glaciation in the Eastern Cape would require a climate 10-
67 17°C colder than present (Lewis and Illgner, 2001) — a magnitude inconsistent with
68 the reconstructed climate change in Lesotho.

69

70 In addition to proposed low elevation glaciation, a relict rock glacier has also been
71 described from the Eastern Cape Drakensberg, suggesting the presence of permafrost
72 at 1800 m asl (Lewis and Hanvey, 1993). However, Grab (2002) estimated that
73 permafrost was only present above 3200 m asl in Lesotho. Contemporary periglacial
74 conditions in the Eastern Cape Drakensberg are restricted to areas exceeding 2765
75 m asl (Kuck and Lewis, 2002), and it is assumed that the last time that extensive

76 periglacial and glacial conditions occurred is during the Last Glacial Maximum (LGM),
77 which is defined as the period of maximum global ice volume (21 ± 2 ka; Mix et al.,
78 2001). Climate proxy records for this period are relatively scarce for southern Africa
79 because of the semi- and hyperarid climates not being conducive to the preservation
80 of long-term palaeoenvironmental records (Chase, 2009). Those that do exist broadly
81 suggest that temperatures were lower than present by 5-7°C (Heaton et al., 1986;
82 Talma and Vogel, 1992; Holmgren et al., 2003), and a study in Lesotho using a glacier
83 reconstruction and mass balance modelling approach suggested that glaciers could
84 have existed there under these temperature reductions (Mills et al., 2012). Estimates
85 of palaeoprecipitation are more problematic, and the climate of southern Africa has
86 previously been considered as drier during the LGM (Partridge, 1997; Holmgren et al.,
87 2003). However, more recent research has suggested that there may have been a
88 shift in the rainfall zones allowing for increased precipitation in some areas during this
89 time (Stuut et al., 2004; Chase and Meadows, 2007; Gasse et al., 2008; Brook et al.,
90 2010; Mills et al., 2012; Scott et al., 2012). The extent of the shift of the rainfall zones
91 is still poorly constrained by data, and a northward shift in the westerly wind belt would
92 have increased the influence of the westerlies in the climate of South Africa (Chase
93 and Meadows, 2007; Mills et al., 2012).

94

95 This paper aims to resolve the controversy regarding the extent of glaciation and cold
96 climate processes in the Eastern Cape Drakensberg. We present the first surface
97 exposure ages for cold climate landforms in southern Africa. Exposure dating provides
98 a way of extending cold climate chronologies beyond glaciated landscapes (Barrows
99 et al., 2004) and testing hypotheses of timing of formation. We also present new
100 geomorphological and sedimentological observations of these landforms to determine

101 their mode of origin. Finally, this paper will present our findings within the context of
102 the growing literature on late Pleistocene climates of southern Africa to better constrain
103 past temperature changes.

104

105 **2. Study area**

106 The Eastern Cape Drakensberg mountains are situated close to the Lesotho border
107 (Fig. 1), and the highest peak in this region is 3001 m asl at Ben Macdhui. The geology
108 of the region is composed of Beaufort and Stormberg Group sandstones and
109 argillaceous rocks with basaltic lavas of the Drakensberg Formation occurring at
110 higher elevations. These basaltic lavas are interbedded with sandstones, pyroclastic
111 rocks, tuffs, and agglomerates (Geological Survey, 1983). These largely flat-lying units
112 exert a strong control on the topography of the region. Mean annual air temperature
113 (MAAT) at 2788 m asl is $\sim 7.5^{\circ}\text{C}$, although this is based on a limited record (1995/1996;
114 Kück and Lewis, 2002). Freeze-thaw cycles are common at these elevations and occur
115 on over 40% of days between May and September with an average of 63 frost days
116 per annum (Kück and Lewis, 2002). The Eastern Cape Drakensberg falls within the
117 summer precipitation zone of southern Africa, where over 66% of precipitation falls
118 between April and September (Tyson and Preston-Whyte, 2000). Very few
119 precipitation records exist and the WorldClim data set estimates precipitation at Ben
120 Macdhui is ~ 940 mm/a (Hijmans et al., 2005).

121

122 *2.1. Site descriptions*

123 Putative glacial landforms were investigated at Mount Enterprise and Killmore along
124 with a possible relict rock glacier in the Bottelnek Valley (Fig. 1). These sites were
125 selected based on previous studies that described the presence of glacial or near

126 glacial conditions. A blockstream at Tiffendell was also investigated, and additional
127 sites were examined at Carlisle's Hoek, along the Bokspruit, and at Moshesh's Ford
128 to determine the lowest altitudinal limit of periglacial activity (Fig. 1).

129

130 Mount Enterprise reaches a maximum elevation of 2565 m asl, and the study site is
131 located at 31.176° S, 27.980° E. Steep cliffs are located below the main peak, with
132 their upper limits at ~2280 m asl. Ridges occurring between 2000 and 2100 m asl have
133 been described by Lewis and Illgner (2001) as moraines (Fig. 2A). These ridges range
134 from 120 to 250 m in length and are no more than 5 m in height. Lewis and Illgner
135 (2001) undertook sedimentological analyses from within one of the ridges and a
136 section, where they describe a diamicton, with the presence of clasts with occasional
137 striations as indicative of glacial transport.

138

139 The Tiffindell area is located on a high plateau and hosts the highest peak in South
140 Africa (Ben Macdhui) and the Tiffindell ski resort (Fig. 2B). The study area is located
141 at 30.653° S, 27.937° E, and the region contains numerous periglacial deposits in the
142 form of blockstreams, stone garlands, patterned ground, and gelifluction terraces.
143 Kück and Lewis (2002) describe active gelifluction terraces occurring at altitudes
144 between 2765 and 2855 m asl at Tiffindell. They measured temperature at ground
145 level during the winter months and found that a diurnal range of over 10°C was not
146 unusual (Kück and Lewis, 2002). Sorted polygons actively form at altitudes exceeding
147 2900 m asl on summit areas that are free of vegetation (Kück, 1996). The stone
148 garlands and blockstreams are not presently active.

149

150 The Killmore site is located in the Bokspruit Valley (Fig. 1) at 30.948° S, 27.941° E and
151 the highest peak is 2324 m asl. A 'bench' occurs on both sides of the valley at an
152 elevation of ~2100 m asl and is formed by a concealed, more resistant layer of basalt
153 (Geological Survey, 1983). Located on the bench on the western side of the valley is
154 an accumulation of boulders that were initially described as a pronival rampart by
155 Lewis (1994; Fig. 2C). This was later reinterpreted as a moraine ridge (Lewis, 2008b),
156 based on the distance from the ridge crest to the backwall being greater than that
157 proposed for pronival ramparts.

158

159 The Bottelnek region is an east-west trending valley drained by the Bottelnekspruit,
160 with peaks reaching elevations >2300 m asl. Sediment accumulations occur along the
161 walls of this valley, and Lewis and Hanvey (1993) suggested that some of these
162 resembled relict rock glaciers. Organic material sampled from within one of the
163 landforms described as a rock glacier in the Rose Hill area produced a radiocarbon
164 date of 21,000 ± 400 ¹⁴C YBP, indicating that the sediment was deposited at or
165 subsequent to this date (Lewis and Hanvey, 1993). The valley is composed of Clarens
166 sandstone, with basalt occurring in the upper catchment and fluvial incision by the
167 Bottelnekspruit exposing several sections through these units. We focus on the Rose
168 Hill deposit located at 31.109° S, 27.777° E (Fig. 2D) that is proposed by Lewis and
169 Hanvey (1993) to have the morphology (lobate / tongue-like feature) and
170 sedimentology of a rock glacier.

171

172 Numerous periglacial deposits occur throughout the Eastern Cape Drakensberg,
173 several of which have been described in detail by Lewis (2008b). Our study includes
174 three additional locations where sections have been exposed in road cuttings at

175 Carlisle's Hoek (30.784° S, 27.970° E), Bokspruit (30.916° S, 27.920° E) and
176 Moshesh's Ford (30.851° S, 27.781° E) (Fig. 1). The Carlisle's Hoek and Bokspruit
177 sites are both underlain by Clarens sandstone, whereas Moshesh's Ford is a basaltic
178 vent fill within the Clarens Formation (Lock et al., 1974).

179

180 **3. Methods**

181 Exposure dating was undertaken at suitable sites at Mount Enterprise and at Tiffindell;
182 whilst the geomorphology was mapped at all sites, and the sedimentology of the
183 deposits was described. At Mount Enterprise we targeted two ridges and a boulder
184 terrace for surface exposure dating, collecting 11 samples in total. We sampled the
185 largest boulders (most blocks sampled were 2-3 m long) along ridge crests to reduce
186 the risk of exhumation through erosion. This site is backed by a high cliff, and therefore
187 we consider risks associated with inheritance to be low. The blockstream at Tiffindell
188 presented a challenge for exposure dating. The source area for blocks was restricted
189 to low cliffs only a few metres high, 150 m above the deposit. Blocks have moved
190 downslope to accumulate in the drainage line. Consequently, inheritance is more likely
191 at this site, and ages are maximum ages for the formation of the deposit. We collected
192 four samples in a longitudinal transect down the deposit to detect any age variations
193 along its length.

194

195 The rock type at both sites was basalt, and so we chose to analyse the cosmogenic
196 nuclide ^{36}Cl . Site information is presented in Table 1. The abundance of major target
197 elements for ^{36}Cl production was determined using X-ray fluorescence. The
198 concentrations of trace elements with large neutron capture cross sections (B, Gd,
199 and Sm) and neutron-producing elements (U and Th) were measured by inductively

200 coupled plasma mass spectrometry. Chlorine content was determined by isotope
201 dilution. The isotopic ratio of $^{36}\text{Cl}/\text{Cl}$ was measured by accelerator mass spectrometry
202 on the 14UD accelerator at the Australian National University (Fifield et al., 2010).
203 Chemical data are available on request.

204

205 Chlorine-36 exposure ages are calculated as detailed in Barrows et al. (2013). We
206 calculated total production from spallation on K, Ca, Ti, and Fe and from muon capture
207 on K and Ca, using the production rates of Stone et al. (1996a, 1996b, 1998), Evans
208 (2001), and Masarik and Reedy (1995). For ^{36}Cl production by neutron capture on K
209 and Cl, we followed the procedures of Liu et al. (1994), Phillips et al. (2001), and Stone
210 et al. (1998) and calculated the nucleogenic contribution following Fabryka-Martin
211 (1988). Production rates were scaled using the scheme of Stone (2000). All
212 measurement errors, including production rate errors, are fully propagated on
213 individual ages. No correction for weathering was applied. All ages are reported at one
214 standard deviation.

215

216 **4. Results**

217 *4.1. Mount Enterprise*

218 The geomorphological map for this site is presented in Fig. 3. We identify two distinct
219 vegetated linear ridges (A and B) between 2000 and 2100 m asl that have large basalt
220 boulders up to 6 m in length on their surface. Ridge A is ~250 m in length, whilst ridge
221 B is ~150 m in length. A further ridge (C) is located to the south where a road cut
222 exposes a section (3). Boulder deposits (D and E) are located on a bench between
223 2100 and 2200 m asl. Talus slopes, boulder terraces, and landslide deposits also

224 occur in close proximity to the linear ridges, indicating that this area is
225 geomorphologically active.

226

227 We present a sedimentological log of several exposed sections at this site in Fig. 4.
228 Section 1 is ~10 m high and is not associated with a distinct ridge. This is the same
229 section that Lewis and Illgner (2001) described as 'till'. The lower unit is ~6 m thick
230 and is a massive matrix-supported diamicton with a fine interbed containing small
231 clasts, dipping at ~35°. The clasts within the diamicton are subrounded to subangular
232 and deeply weathered, usually with spheroidal onion skin weathering. The unit is
233 crudely graded with much larger blocks in the lower parts of the unit, below the dipping
234 interbed. The upper 3 m of the section is composed of alternating units of matrix-
235 supported subangular to angular clasts, which are oriented downslope, and fine-
236 grained layers of silty clay, which may reflect two buried palaeosols. A mixture of
237 sandstone and basalt clasts occurs in all units.

238

239 Section 2 (Figs. 3 and 4) consists of a highly weathered lower unit with the presence
240 of weathered core-stones, underlying an ~2-m-thick matrix-supported diamicton with
241 clasts up to ~1 m in length. The lower unit correlates with section 1 and consists of a
242 matrix-supported diamicton with blocks up to ~1.5 m in length. Many of the larger
243 clasts have undergone onion skin weathering and have completely weathered in situ
244 in some instances (Fig. 5). Weathering rinds are up to 12 cm in this lower unit. The
245 upper unit is composed of angular clasts within a finer-grained matrix, and weathering
246 rinds in this unit are <10 mm. The relatively high degree of weathering in the lower unit
247 of the two sections in comparison to the upper unit is likely to represent great antiquity.

248

249 No sections dissect ridges A and B; however a section (3) is exposed through ridge C
250 (Fig. 4). This section is ~2.5 m thick and is composed of ~1.25 m of highly weathered
251 bedrock, with the presence of deeply weathered corestones, overlain by 1.0 m of
252 matrix-supported diamicton. The diamicton unit is divided by a weakly developed
253 palaeosol that is ~10 cm deep. Clasts within the diamicton range from a few
254 centimetres to ~1.0 m and are predominantly angular to subangular. Ridge C is
255 therefore bedrock-cored with a surficial layer of sediment.

256

257 The exposure ages obtained from ridges A and B and the boulder terrace are
258 presented in Table 2. The bulk of the ages are much younger than the age previously
259 suggested by Lewis and Illgner (2001) for these features. The two ridges and boulder
260 terrace are distinctly separated in time without obvious evidence for inheritance. The
261 boulder terrace was deposited between 5.0 ± 0.3 and 7.7 ± 0.4 ka, with an average
262 age of 6.8 ± 1.5 ka ($X^2 = 22$). Below this feature, the upper ridge (A) has exposure
263 ages between 9.2 ± 0.3 and 12.0 ± 0.7 ka with a mean age of 10.5 ± 1.2 ka ($X^2 = 3.7$).
264 The lowest ridge (B) has two ages with a mean of 19.0 ± 2.1 ka ($X^2 = 3.6$). A third age
265 (11.15 ± 0.58 ka) is similar in age to the upper ridge. This difference might be
266 accounted for by the boulder rolling onto the lower ridge when the upper ridge was
267 deposited.

268

269 4.2. Tiffindell

270 The slopes in this region are south-facing and are conducive to the preservation of
271 late-lying snow as illustrated in the satellite image (Fig. 6A). The study site has
272 numerous areas where bedrock outcrops, indicating a relatively thin regolith cover,
273 and where moderately low cliffs occur in the upper part of the catchment. A

274 blockstream occurs between 2730 and 2785 m asl and is ~125 m in length and up to
275 15 m in width. The blocks that make up the blockstream are up to 2 m in length and
276 show no preferred orientation. The blocks in the upper part of the blockstream are
277 predominantly angular to subangular, becoming slightly more subrounded toward the
278 lower areas. Ages obtained from blocks within the blockstream (Table 2) range from
279 12.7 ± 0.8 to 49.3 ± 2.5 ka. Samples were taken from the largest blocks with an
280 unobstructed horizon in a transect along the blockstream. The two youngest ages
281 overlap and have an average age of 13.1 ± 0.6 ka ($X^2 = 6.7$), which probably
282 represents the time of stabilisation and suggests that the blockstream was active at
283 the end of the Pleistocene. The scatter in the ages most likely reflects inheritance.

284

285 *4.3. Killmore*

286 A distinct ridge, ~500 m in length, is a prominent feature in the landscape below near
287 vertical cliffs, which trend N-S (Fig. 7). The lithology here is vulnerable to physical
288 weathering, and vertical cracks and column structures can be observed in the basalt
289 cliff walls. The interbedded basaltic lavas in this area, which form layers of different
290 strength characteristics, could also make this area prone to landsliding. Below these
291 cliffs are vegetated fans and talus cones that occur along the length of the cliff. The
292 ridge surface is subdued and almost flat toward its northern limits, and many large
293 basalt boulders sit on and inside the ridge. A likely great age for these blocks is
294 indicated by thick weathering rinds and some blocks are disintegrating in situ (e.g., Fig.
295 8), indicating that they are significantly older than those sampled from Mount
296 Enterprise. Blocks making up the talus slopes inside the ridge are more angular and
297 less weathered. Vesicles (usually infilled) occur as layers in the boulders and provide
298 a 'way-up' criterion for determining the original orientation of the blocks. The dip and

299 strike of these layers was measured for 21 boulders in a boulder-rich, partly enclosed
300 shallow depression of the ridge. In more than 75% of cases, the dip of the layers shows
301 a significant orientation preference where the boulders have undergone rotation
302 through $>75^\circ$, from vertical to nearly flat-lying (Fig. 7C); whereas the layers are also
303 preferentially oriented in an easterly direction, which is perpendicular to the cliff face.

304

305 *4.4. Rose Hill*

306 The landform that we focus on in this area is located adjacent to Rose Hill farm (Fig.
307 9) and was previously interpreted as a rock glacier by Lewis and Hanvey (1993). The
308 landform is not very distinct, although it has a lobate form in the lower part of the
309 catchment that has been incised by fluvial activity. There is evidence of contemporary
310 channel incision in the upper part of the catchment, most likely as a result of high-
311 energy seasonal flow and snowmelt. In the lower parts of the catchment below ~2050
312 m asl, numerous locations with sandstone outcrops suggest that the regolith is locally
313 thin. In August of 2011 a debris flow occurred, covering almost the entire lobate section
314 of the 'rock glacier'. This debris flow accumulation spans an altitudinal range from 1950
315 to 2000 m asl and terminates as a series of 'fingers' that almost reach the river. The
316 debris flow has a broad body up to 50 m across with boulders up to 1 m in diameter,
317 intermixed with finer material. Clasts transported by the debris flow show linear impact
318 / percussion marks, where clast collision has occurred during transport.

319

320 Fluvial incision by the Bottelnekspruit has exposed a section through the 'rock glacier'
321 that is ~12 m high (Fig. 4). Bedrock comprised of Clarens sandstone forms the base
322 of the section and is overlain by a diamicton composed of small, flat, angular clasts
323 showing preferred orientation downslope, within a fine-grained matrix. The clasts in

324 this unit are sandstone, which suggests a local source from the bedrock. Overlying
325 this unit is a diamicton with larger clasts and increasing amounts of basalt up profile,
326 indicating increasing input from the upper catchment. Within the diamicton are
327 intercalated, clast-supported alluvial units up to 10 cm in thickness, consisting of
328 pebbles with very little fine matrix material. The upper unit is dominated by basalt and
329 contains large clasts up to 2 m in length within a fine-grained matrix. A clast-supported
330 bed is also present within this unit.

331

332 *4.5. Periglacial deposits*

333 The sections we studied at Carlisle's Hoek (1838 m asl) and Bokspruit (1844 m asl)
334 are very similar and therefore we only present the section from Carlisle's Hoek (Fig.
335 4). Both sections are comprised of basal sandstone bedrock, overlain by a unit of flat
336 clasts up to 15 cm in length, showing a strong preferred orientation in a southwesterly
337 direction, which conforms to the direction of the slope. A silty unit underlies the
338 present-day soil. At Moshesh's Ford (1740 m asl), there are alternating units of larger
339 blocks (up to 30 cm) within a finer-grained matrix and finer sediments that are clast
340 supported. Here the source material is columnar basalt, which has very small, thin
341 columns and is more susceptible to fracturing. The clasts show no preferred
342 orientation.

343

344

345 **5. Discussion**

346 *5.1. Site interpretation*

347 At Mount Enterprise we could find no direct evidence for glacial activity, and our
348 observations indicate that an alternate model can explain the geomorphology in this

349 area. The site itself is not situated in a location that would be more conducive to
350 glaciation than other sites in this region. Areas of contemporary late-lying snow occur
351 preferentially on the higher south-facing slopes in this region, as observed in the field
352 and where depositional ridges are absent. The Mount Enterprise ridges superficially
353 resemble moraines but are not crescentic as expected for an ice source from the
354 direction of the cliffs. The lowermost ridge (B) and the ridge that has been exposed by
355 the road (C) are composed of sheets of diamicton that we propose are the result of
356 accumulation of colluvium through processes of landsliding and debris flows. The
357 diamicton sheets suggest various periods of enhanced mass movement activity and
358 multiple episodes of debris flow activity. The differences in weathering rind thickness
359 suggest that these processes have been ongoing for a substantial amount of time.
360 Subsurface weathering rinds of 4-10 cm in dolerite are known to be at least mid-
361 Pleistocene in age in a similar climate in Tasmania (Kiernan, 1990), which is similar to
362 those measured in the lower unit in sections 1 and 2 (Fig. 4). Debris flows are likely to
363 have been more frequent during the LGM when late-lying snow would have been more
364 extensive beneath the cliffs and when the ages obtained from the lower of the two
365 ridges (B) probably indicate mass movement during this time period. However, ridge
366 A and the boulder terrace were constructed about 10,000 years after the peak of the
367 LGM, during a warm climate interval. The landscape here has therefore been
368 generated by a series of rockfall, landslides, and debris flows, continuing to the present.
369 Although striated clasts have been described from this site (Lewis and Illgner, 2001),
370 these striae are not typical of glacial striae and match impact / percussion marks as
371 observed on the recent debris flow at Rose Hill, reflecting clast collision during
372 transport (Caballero et al., 2014). The burial of these clasts has allowed for the
373 preservation of these impact marks.

374

375 The Killmore site also only superficially resembles a glaciated site. The section
376 examined had a distinct ridge and a potential catchment for a small glacier / snow
377 patch under the steep cliffs. However, no evidence of former meltwater streams exists
378 and blocks show no evidence of transport by ice. Boulders are located on the proximal
379 side of the ridge, suggesting that they have originated from rockfall. The orientation of
380 these blocks perpendicular to the cliff face indicates that this feature most likely
381 represents a series of rotational landslides or topples. The heterogeneity of the site's
382 geology, comprised of different strength rocks such as basaltic lava, sandstone, tuff,
383 and agglomerate, would make this particular area prone to landsliding. Rockfalls are
384 among the most common type of slope movement in mountain regions worldwide
385 (Whalley, 1984; Flageollet and Weber, 1996) and the occurrence of numerous talus
386 slopes along the cliff face suggests that these processes are very active in this region.
387 Falls and topples occur where sufficiently steep slopes exist (van Beek et al., 2008),
388 and the near-vertical cliffs in some areas would make them conducive to such
389 processes. Vertical weaknesses in the bedrock create columns, such as those
390 observed on both sides of the valley at Killmore, which subsequently fail (Dikau et al.,
391 1996). Movement would have been arrested as a result of the width of the bench and
392 reduction in slope angle, allowing retention of the mass on the bench and creating
393 reverse slope back to the cliff. This area is at a significant altitude (>2000 m asl),
394 therefore freeze-thaw cycles could also have been important over long timescales for
395 weathering the rock prior to the occurrence of mass movement processes. The long-
396 term effect of climate in weakening the rock through weathering must be considered
397 as an important driving force of toppling processes (Dikau et al., 1996). Boulder

398 accumulations also occur on the bench on the opposite side of the valley, indicating
399 that these processes are common in the region.

400

401 The Rose Hill site has a few features in common with rock glaciers, including its
402 elongated profile and its thickness (Lewis and Hanvey, 1993). Rock glaciers are lobate
403 or tongue-shaped landforms of frozen material (French, 2007), originating either as
404 gradually creeping permafrost and ice-rich debris on nonglacierised slopes, or as
405 debris-covered remnant glaciers in permafrost-free areas (Haeberli et al., 2006). They
406 would therefore imply the presence of either permafrost or glacial ice. The Rose Hill
407 landform has been interpreted as a relict rock glacier based on its morphology,
408 stratigraphy, particle size, clast characteristics, and morphology of quartz grains
409 (Lewis and Hanvey, 1993). A clear distinction between coarse debris overlying fine
410 debris was identified, which commonly occurs in rock glaciers (Lewis and Hanvey,
411 1993). However, Zurawek (2003) suggested that this two-layered stratigraphy must be
412 considered within a geomorphological context and that it should not be regarded as a
413 prerequisite condition for the presence of a relict rock glacier. In fact, Zurawek (2003)
414 stated that sedimentological properties are largely controlled by the source lithology
415 and are of little value in identifying relict rock glaciers.

416

417 The rock glacier origin of the landforms found in the Bottelnekspruit region have
418 recently been questioned by Grab (2000), who proposed that the morphology and
419 sedimentology of some of the landforms may represent debris flow and solifluction
420 processes. The Rose Hill landform has a number of features that indicate that it cannot
421 be a rock glacier. Firstly, the lobate form contains several areas that are bedrock,
422 exposed where the soil is thin. The overall topography of the western side of the

423 feature is governed by the underlying bedrock. Secondly, the internal structure of the
424 Rose Hill feature does not clearly contain the two-layered stratigraphy proposed to be
425 typical of a rock glacier. The lower sedimentary unit in the exposed face has a
426 preferred orientation downvalley, indicative of solifluction processes (Nelson, 1985)
427 acting upon locally derived sandstone, in the wrong direction for material originating
428 from the catchment. The overlying unit is comprised of a series of debris flows with no
429 clast-supported layer at the surface typical of rock glaciers. The interbedded alluvial
430 units indicate that the sequence was accumulated sequentially and that the stream
431 once flowed at a much higher base level during accretion. The upper parts of the
432 catchment contain several avalanche couloirs, where snow likely accumulates under
433 contemporary conditions. Greater snow accumulation during colder conditions and
434 associated spring melt would enhance slope instability and increase the frequency of
435 debris flows. Based on this evidence, we propose that the Rose Hill landform reflects
436 an accumulation of sediment as a result of mass movement processes such as
437 solifluction and debris flows over time with interbedded alluvial units.

438

439 The ages obtained from the blockstream at Tiffindell indicate that this was active
440 during the last glaciation and ceased moving at the end of the Pleistocene. Tiffindell
441 hosts the highest peak in South Africa, the slopes are south-facing, and this area
442 retains the largest amount of late-lying snow in the region, yet glacial deposits are
443 absent. The complete absence of glacial deposits, in possibly the most likely location
444 in South Africa, is indirect evidence against glaciation at other less favourable sites
445 such as Mount Enterprise. The extensive relict periglacial deposits as well as the dated
446 blockstream, suggest that this was a periglacial environment during the late
447 Pleistocene. Deep seasonal frost would have been necessary in order for mass

448 wasting processes associated with frost creep and block movement to take place. A
449 similar deposit has been described by Boelhouwers et al. (2002) in the Lesotho
450 Highlands at 3000-3200 m asl. This landform is much more extensive (>1 km in length)
451 than those observed in the Eastern Cape, but it has also been attributed to the
452 occurrence of deep seasonal frost and restricted snow cover during the LGM. The
453 dated blockstream at Tiffindell has a slightly younger age than similar dated periglacial
454 deposits in a similar climate in Australia (Barrows et al., 2004), where most periglacial
455 activity occurred during the LGM.

456

457 *5.2. Palaeoclimatic implications*

458 Rock glaciers typically form in areas where the mean annual air temperature (MAAT)
459 is $\leq -2^{\circ}\text{C}$ (Humlum, 1998). Therefore, Lewis (2008c) suggested that in order for rock
460 glaciers to exist at 1800 m asl in the Eastern Cape Drakensberg, a temperature drop
461 of $17\text{-}19^{\circ}\text{C}$ would be necessary during the LGM. In addition, for a glacier to have
462 existed at Mount Enterprise, temperatures would have had to have been at least 10°C
463 below present (Lewis and Illgner, 2001). The reevaluation of the cold-climate
464 landforms in the Eastern Cape Drakensberg and the absence of evidence for
465 glaciation has important implications for the palaeoclimate in this region. There is
466 evidence that humans abandoned high altitude sites in this region from ~ 24 to 12 ka,
467 most likely because of harsh climatic conditions (Lewis, 2008c). Climate data obtained
468 from the South Africa weather bureau (Lewis and Illgner, 2001) indicates that at
469 Rhodes (1676 m asl), MAAT is 11.8°C , and the coldest four-month average is 6.3°C .
470 This suggests that a temperature depression of $6\text{-}7^{\circ}\text{C}$ would allow for the duration and
471 cyclic pattern of ground temperatures passing below 0°C to be much more frequent at
472 elevations above 1700 m asl, which is in accordance with proxy records suggesting a

473 5-7°C temperature depression during the LGM (Heaton et al., 1986; Talma and Vogel,
474 1992; Scott, 1999; Holmgren et al., 2003).

475

476 Our proposed temperature depression of 6-7°C for the Eastern Cape Drakensberg
477 also agrees with the distribution of widespread slope deposits that have been
478 described by Lewis (2008b). In fact, Lewis (2008c) suggested that these would have
479 formed when temperatures were ~6°C below present. However, he proposed that
480 these deposits would have formed subsequent to the colder conditions when the rock
481 glaciers were active. In addition, findings from the adjacent Lesotho Highlands also
482 suggest that temperatures would have been in the order of ~6°C colder during the
483 LGM. The evidence of small-scale niche glaciers during the LGM in eastern Lesotho
484 has been described by Mills and Grab (2005) and Mills et al. (2009a,b, 2012).
485 Moraines have been identified based on morphological, sedimentological, and
486 micromorphological evidence; and ages obtained using soil organic matter from within
487 the moraines range from ~14 to 20.5 cal ka (Mills et al., 2009a). Mass balance
488 modelling of the former glaciers (Mills et al., 2012) suggests that this region could have
489 sustained small glaciers based on a 6°C temperature depression. If a 10-17°C
490 temperature drop had occurred, as suggested by Lewis and Illgner (2001), then this
491 would imply that much more extensive glaciation would have occurred in the Lesotho
492 Highlands. In addition, the presence of a relict rock glacier at 1800 m asl in the Eastern
493 Cape Drakensberg would imply that permafrost would have also occurred at higher
494 elevations; however, evidence for Pleistocene permafrost (large sorted patterned
495 ground) only exists at elevations exceeding 3450 m asl in Lesotho (Grab, 2002).

496

497 The 6-7°C temperature depression suggested for the Eastern Cape Drakensberg
498 during the LGM is not only in keeping with temperature depressions suggested for the
499 wider southern African region but also other areas in the Southern Hemisphere, such
500 as Australia and South America. A temperature depression of 8-9°C has been
501 suggested for the LGM over mainland Australia and about 6°C for Tasmania (Galloway,
502 1965; Williams et al., 2009), whilst modelling results for southern Patagonia agree with
503 a 6°C temperature depression during the LGM (Kaplan et al., 2008).

504

505 **6. Conclusion**

506 We have reevaluated the cold climate landforms in the Eastern Cape Drakensberg,
507 and we present cosmogenic nuclide exposure ages from these landforms in order to
508 determine the timing for their emplacement and obtain a better understanding of the
509 process of landscape development. We find that glaciers were absent in the Eastern
510 Cape Drakensberg during the LGM. The ages obtained from Mount Enterprise suggest
511 a complex landscape history, reflecting the accumulation of colluvium through
512 processes of landsliding and debris flow, creating ridges. The ages obtained from the
513 Tiffindell blockstream indicate emplacement during the late Pleistocene, when
514 temperatures were cold enough to permit the development of deep seasonal ice. The
515 reevaluation of the Mount Enterprise, Rose Hill, and Killmore sites — along with the
516 evidence from Tiffindell and periglacial deposits at lower elevations — indicates that
517 periglacial conditions prevailed during the LGM, with temperature depressions of ~6°C,
518 allowing for enhanced periglacial activity and mass movement processes.

519

520 **Acknowledgements**

521 This work was funded by the Royal Geographical Society Peter Fleming Award,
522 awarded jointly to SM and TB. We thank the department of Rural Development and
523 Land Reform for the provision of the 2009 rectified 0.5 m aerial imagery, all the
524 landowners who kindly allowed us access to their land, and Dave Walker from
525 'Walkerbouts Inn' and Wikus Roodt for the help they provided in tracking down the
526 details of all the landowners. We would also like to thank Colin Lewis for valuable
527 comments on a draft of the manuscript as well as Prof Jasper Knight and an
528 anonymous reviewer.

529

530

531 **References**

532 Barrows, T.T., Stone, J.O., Fifield, L. K., 2004. Exposure ages for Pleistocene
533 periglacial deposits in Australia. *Quaternary Science Reviews* 23, 697-708.

534 Barrows, T.T., Almond, P., Rose, R., Fifield, L.K., Mills, S.C., Tims, S.G. 2013. Late
535 Pleistocene glacial stratigraphy of the Kumara-Moana region, West Coast of South
536 Island, New Zealand. *Quaternary Science Reviews* 74, 139-159.

537 Boelhouwers, J.C., Holness, S., Meiklejohn, K.I., Sumner, P. D., 2002. Observations
538 on a blockstream in the vicinity of Sani Pass, Lesotho highlands, southern Africa.
539 *Permafrost and Periglacial Processes* 13, 251-257.

540 Brook, G.A., Scott, L., Railsback, L.B., Goddard, E.A., 2010. A 35 ka pollen and
541 isotope record of environmental change along the southern margin of the Kalahari
542 from a stalagmite and animal dung deposits in Wonderwerk Cave, South Africa.
543 *Journal of Arid Environments* 74, 870-884.

544 Caballero, L., Sarocchi, D., Soto, E., Borselli, L., 2014. Rheological changes induced
545 by clast fragmentation in debris flows. *Journal of Geophysical Research: Earth*
546 *Surface*. 119, 1800-1817.

547 Chase, B. M., 2009. Evaluating the use of dune sediments as a proxy for palaeo-
548 aridity: A southern African case study. *Earth Science Reviews*. 93, 31-45.

549 Chase, B.M., Meadows, M.E., 2007. Late Quaternary dynamics of southern Africa's
550 winter rainfall zone. *Earth Science Reviews* 84, 103-138.

551 Dikau, R., Schrott, L., Dehn, M., 1996. Topple. In: Dikau, R., Brunsden, D., Schrott,
552 L. and Ibsen, M-L. (Eds). *Landslide recognition: Identification, movement and*
553 *causes*. John Wiley & Sons Ltd. Chichester. 29-41.

554 Evans, J.M., 2001. Calibration of the production rates of cosmogenic ^{36}Cl from
555 potassium. PhD thesis, The Australian National University, Canberra.

556 Fabryka-Martin, J.T., 1988. Production of radionuclides in the Earth and their
557 hydrogeologic significance, with emphasis on chlorine-36 and iodine-129.
558 Unpublished PhD thesis, The University of Arizona.

559 Fifield, L.K., Tims, S.G., Fujioka, T., Hoo, W.T., Everett, S.E., 2010. Accelerator
560 mass spectrometry with the 14UD accelerator at the Australian National University.
561 *Nuclear Instruments and Methods in Physics Research Section B: Beam Interactions*
562 *with Materials and Atoms* 268, 858-862.

563 Flageollet, J. C., Weber, D., 1996. Fall. In: Dikau, R., Brunsden, D., Schrott, L.,
564 Ibsen, M. L. (Eds.). *Landslide recognition*. John Wiley and Sons Ltd, Chichester.

565 French, H. M., 2007. The periglacial environment. John Wiley and Sons Ltd,
566 Chichester.

567 Galloway, R.W., 1965. Late Quaternary Climates in Australia. The Journal of
568 Geology 73, 603-618.

569 Gasse, F., Chalie, F., Vincens, A., Williams, M.A.J., Williamson, D., 2008. Climatic
570 patterns in equatorial and southern Africa from 30,000 to 10,000 years ago
571 reconstructed from terrestrial and near-shore proxy data. Quaternary Science
572 Reviews 27, 2316-2340.

573 Geological Survey., 1983. 1:250,000 geological series, 3026 Aliwal North.
574 Department of Mineral and Energy Affairs, Pretoria.

575 Grab, S.W., 1996. Debris deposits in the high Drakensberg, South Africa: Possible
576 indicators for plateau, niche and cirque glaciation. Zeitschrift für Geomorphologie,
577 Supplementbände 103, 389-403.

578 Grab, S.W., 2000. Periglacial features. In: Partridge, T.C., Maud, R.R. (Eds). *The*
579 *Cenozoic of southern Africa*. Oxford University Press, Oxford. 207-217.

580 Grab S.W., 2002. Characteristics and palaeoenvironmental significance of relict sorted
581 patterned ground, Drakensberg plateau, southern Africa. Quaternary Science
582 Reviews 21, 1729-1744.

583 Haeberli, W., Hallet, B., Arenson, L., Elconin, R., Humlum, O., Käab, A., Kaufmann,
584 V., Ladanyi, B., Matsuoka, N., Springham, S., Vonder Mühl, D., 2006. Permafrost
585 creep and rock glacier dynamics. Permafrost and periglacial processes 17, 189-214.

586 Hall, K., 2010. The shape of glacial valleys and implications for southern African
587 glaciation. *South African Geographical Journal* 92, 35-44.

588 Heaton, T.H.E., Talma, A.S., Vogel, J.C., 1986. Dissolved gas palaeotemperatures
589 and ^{18}O variations derived from groundwater near Uitenhage, South Africa.
590 *Quaternary Research* 56, 79-88.

591 Hijmans, R.J., Cameron, S.E., Parra, J.L., Jones, P.G., Jarvis, A., 2005. Very high
592 resolution interpolated climate surfaces for global land areas. *International Journal of*
593 *Climatology* 25, 1965-1978.

594 Holmgren, K., Lee-Thorp, J.A., Cooper, G.R.J., Lundblad, K., Partridge, T.C., Scott,
595 L., Sitaldeen, R., Talma, A.S., Tyson, P.D., 2003. Persistent millennial-scale
596 climatic variability over the past 25,000 years in Southern Africa. *Quaternary Science*
597 *Reviews* 22, 2311-2326.

598 Humlum, O., 1998. The climatic significance of rock glaciers. *Permafrost and*
599 *periglacial processes* 9, 375-395.

600 Kaplan, M.R., Fogwill, C.J., Sugden, D.E., Hulton, N.R.J., Kubik, P. W., Freeman,
601 S.P.H.T., 2008. Southern Patagonian glacial chronology for the Last Glacial period
602 and implications for Southern Ocean climate. *Quaternary Science Reviews* 27, 284-
603 294.

604 Kiernan, K., 1990. Weathering as an indicator of the age of Quaternary glacial
605 deposits in Tasmania. *Australian Geographer* 21, 1-17.

606 Kück, K.M., 1996. Periglacial features in the vicinity of Tiffindell Ski Resort, north–
607 east Cape Drakensberg, South Africa, and their implications for the development of
608 the resort. Unpublished M. Sc. thesis, Rhodes University, Grahamstown.

609 Kück, K.M., Lewis, C.A., 2002. Terracettes and active gelifluction terraces in the
610 Drakensberg of the Province of the Eastern Cape, South Africa: a process study.
611 South African Geographical Journal 84, 214–225.

612 Lewis, C.A., 1994. Protalus ramparts and the altitude of the local equilibrium line
613 altitude during the Last Glacial Stage in Bokspruit, East Cape Drakensberg, South
614 Africa. Geografiska Annaler 76A, 37-48.

615 Lewis, C.A., 2008a. Glaciations and Glacial Features. In: Lewis, C.A. (ed).
616 *Geomorphology of the Eastern Cape: South Africa*. NISC, Grahamstown. 127-148.

617 Lewis, C.A., 2008b. Periglacial features. In: Lewis, C.A. (ed). *Geomorphology of the*
618 *Eastern Cape: South Africa*. NISC, Grahamstown. 149-185.

619 Lewis C.A., 2008c. Late Quaternary climatic changes, and associated human
620 responses, during the last ~45000 yr in the Eastern and adjoining Western Cape,
621 South Africa. Earth Science Reviews 88, 167-187.

622 Lewis, C.A., Harvey, P.M. 1993. The remains of rock glaciers in Bottelnek, East Cape
623 Drakensberg, South Africa. Transactions of the Royal Society of South Africa 48, 265-
624 289.

625 Lewis C.A., Illgner P.M. 2001. Late Quaternary glaciation in Southern Africa: Moraine
626 ridges and glacial deposits at Mount Enterprise in the Drakensberg of the Eastern
627 Cape Province, South Africa. Journal of Quaternary Science 16, 365-374.

628 Liu, B., Phillips, F.M., Fabryka-Martin, J.T., Fowler, M.M., Stone, W.D., 1994.
629 Cosmogenic ^{36}Cl accumulation in unstable landforms 1. Effects of the thermal neutron
630 distribution. *Water Resources Research* 30, 3115-3125.

631 Lock, B.E., Paverd, A.L., Broderick, T.J. 1974. Stratigraphy of the Karoo volcanic rocks
632 of the Barkly East district. *Transactions of the Geological Society of South Africa* 77,
633 117-129.

634 Marker, M.E., 1991. The evidence for cirque glaciation in Lesotho. *Permafrost &*
635 *Periglacial Processes* 2, 21-30.

636 Masarik, J., Reedy, R.C., 1995. Terrestrial cosmogenic-nuclide production
637 systematics calculated from numerical simulations. *Earth and Planetary Science*
638 *Letters* 136, 381-395.

639 Mills, S.C., Grab, S.W., 2005. Debris ridges along the southern Drakensberg
640 escarpment as evidence for Quaternary glaciation in southern Africa. *Quaternary*
641 *International* 129, 61-73.

642 Mills, S.C., Grab, S.W., Carr, S.J., 2009a. Late Quaternary moraines along the
643 Sekhokong range, eastern Lesotho: Contrasting the geomorphic history of north- and
644 south-facing slopes. *Geografiska Annaler* 91A, 121-140.

645 Mills, S.C., Grab, S.W., Carr, S.J., 2009b. Recognition and palaeoclimatic
646 implications of late Quaternary niche glaciation in eastern Lesotho. *Journal of*
647 *Quaternary Science* 24, 647-663.

648 Mills, S.C., Grab, S.W., Rea, B.R., Carr, S.J., Farrow, A., 2012. Shifting westerlies
649 and precipitation patterns during the Late Pleistocene in southern Africa determined

650 using glacier reconstruction and mass balance modelling. *Quaternary Science*
651 *Reviews* 55, 145–159.

652 Mix, A.C., Bard, E., Schneider, R., 2001. Environmental processes of the ice age:
653 land, oceans, glaciers (EPILOG). *Quaternary Science Reviews* 20, 627-657.

654 Nelson, F. E., 1985. A preliminary investigation of solifluction macrofabrics. *Catena* 12,
655 23-33.

656 Partridge, T.C., 1997. Cainozoic environmental change in southern Africa, with special
657 emphasis on the last 200 000 years. *Progress in Physical Geography*. **21**. pp. 2-32.

658 Phillips, F.M., Stone, W.D., Fabryka-Martin, J.T., 2001. An improved approach to
659 calculating low-energy cosmic-ray neutron fluxes near the land/atmosphere interface.
660 *Chemical Geology* 175, 689-701.

661 Sanger, H., 1988. Recent periglacial morphodynamics and Pleistocene glaciations of
662 the Western Cape folded belt, South Africa. In *Geomorphological Studies in Southern*
663 *Africa*, Dardis, G.F, Moon, B.P. (Eds.), Balkema: Rotterdam, 383-388.

664 Scott, L., 1999. Vegetation history and climate in the Savanna biome south Africa
665 since 190,000 ka: a comparison of pollen data from the Tswaing crater (the Pretoria
666 Saltpan) and Wonderkrater. *Quaternary International* 57-58, 215-223.

667 Scott, L., Neumann, F.H., Brook, G.A., Bousman, C.B., Norstrom, E., Metwally, A.A.,
668 2012. Terrestrial fossil-pollen evidence of climate change during the last 26 thousand
669 years in Southern Africa. *Quaternary Science Reviews* 32, 100-118.

670 Sparrow, G.W.A., 1967. Southern African cirques and arˆetes. *Journal of Geography*
671 2, 9-11.

672 Stone, J.O., 2000. Air pressure and cosmogenic isotope production. Journal of
673 Geophysical Research 105, 23,753-23,759.

674 Stone, J.O., Allan, G.L., Fifield, L.K., Cresswell, R.G., 1996a. Cosmogenic chlorine-36
675 from calcium spallation. Geochimica et Cosmochimica Acta 60, 679-692.

676 Stone, J.O., Evans, J.M., Fifield, L.K., Cresswell, R.G., Allan, G.L., 1996b.
677 Cosmogenic chlorine-36 production rates from potassium and calcium. Radiocarbon
678 38, 170-171.

679 Stone, J.O.H., Evans, J.M., Fifield, L.K., Allan, G.L., Cresswell, R.G., 1998.
680 Cosmogenic chlorine-36 production in calcite by muons. Geochimica et
681 Cosmochimica Acta 62, 433-454.

682 Stuut, J.B.W., Crosta, X., van der Borg, K., Schneider, R., 2004. Relationship
683 between Antarctic sea ice and southwest African climate during the late Quaternary.
684 Geology 32, 909-912.

685 Talma, A.S., Vogel, J.C., 1992. Late Quaternary paleotemperatures derived from a
686 speleothem from Cango Caves, Cape Province, South Africa. Quaternary Research
687 37, 203-213.

688 Tyson, P.D., Preston-Whyte, R.A., 2000. The Weather and Climate of Southern
689 Africa. Oxford University Press, Oxford.

690 van Beek, R, Cammeraat, E., Andreu, V., Mickovski, S.B., Dorren, L., 2008. Hillslope
691 processes: Mass wasting, slope stability and erosion. In: Norris, J.E., Stokes,
692 A., Mickovski, S.B., Cammeraat, E., van Beek, R., Nicoll, B.C., Achim, A. (Eds.).
693 *Slope stability and erosion control: Echotechnological solutions*. Springer, Dordrecht.

694 Whalley, W. B., 1984. Rockfalls. In: Brunnsden, D. and Prior, D. B. (Eds). *Slope*
695 *Instability*. Wiley, Chichester.

696 Williams, M., Cook, E., van der Kaars, S., Barrows, T., Shulmeister, J. and Kershaw,
697 P., 2009. Glacial and deglacial climatic patterns in Australia and surrounding regions
698 from 35 000 to 10 000 years ago reconstructed from terrestrial and near-shore proxy
699 data. *Quaternary Science Reviews* 28, 2398-2419.

700 Zurawek, R., 2003. The problem of the identification of relict rock glaciers on
701 sedimentological evidence. *Landform Analysis* 4, 7-15.

702

703 **Figure Captions**

704 **Fig. 1.** Location map showing the position of the study sites (1 = Mount Enterprise, 2
705 = Tiffindell, 3 = Killmore, 4 = Rose Hill, 5 = Carlisle's Hoek, 6 = Bokspruit, 7 =
706 Moshesh's Ford).

707

708 **Fig. 2.** Photos of the main study sites at Mount Enterprise (A), Tiffindell (B), Killmore
709 (C) and Rose Hill (D).

710

711 **Fig. 3.** Three-dimensional model of aerial imagery (A) (aerial imagery obtained from
712 the Department of Rural Development and Land Reform (0.5 m ground sample
713 distance) and then draped over 30 m ASTER DEM) and geomorphological map (B)
714 of the Mount Enterprise site showing the sample sites for surface exposure dating.
715 Sites labelled 1-3 are sedimentological descriptions, whilst features labelled A-D are
716 geomorphological landforms described in the text.

717

718 **Fig. 4.** Stratigraphic diagram showing the key sedimentological features at Mount
719 Enterprise, Rose Hill, Carlisle's Hoek, and Moshesh's Ford.

720

721 **Fig. 5.** Weathering rinds observed in the lower unit of section 2 at Mount Enterprise.
722 Note two clasts indicated by arrows that have completely weathered in situ.

723

724 **Fig. 6.** Three-dimensional model of aerial imagery (A) (aerial imagery obtained from
725 the Department of Rural Development and Land Reform (0.5 m ground sample
726 distance) and then draped over 30 m ASTER DEM) and geomorphological map (B)
727 of the Tiffindell site showing the sample sites for surface exposure dating.

728

729 **Fig. 7.** Geomorphological map (A), three-dimensional model of aerial imagery (B)
730 (aerial imagery obtained from the Department of Rural Development and Land
731 Reform (0.5 m ground sample distance) and then draped over 30 m ASTER DEM),
732 and block orientation (C) at the Killmore site. Box in A indicates sampling location for
733 block orientations. Box in B indicates location of study site (A). Note the topographic
734 control from more resistant flat-lying layers as indicated by the arrows in B.

735

736 **Fig. 8.** Photos illustrating the highly weathered nature of the blocks sitting on the
737 surface of the Killmore ridge.

738

739 **Fig. 9.** Three-dimensional model of aerial imagery (A) (aerial imagery obtained from
740 the Department of Rural Development and Land Reform (0.5 m ground sample
741 distance) and then draped over 30 m ASTER DEM) and geomorphological map (B)
742 of the Rose Hill site.

Figure 1

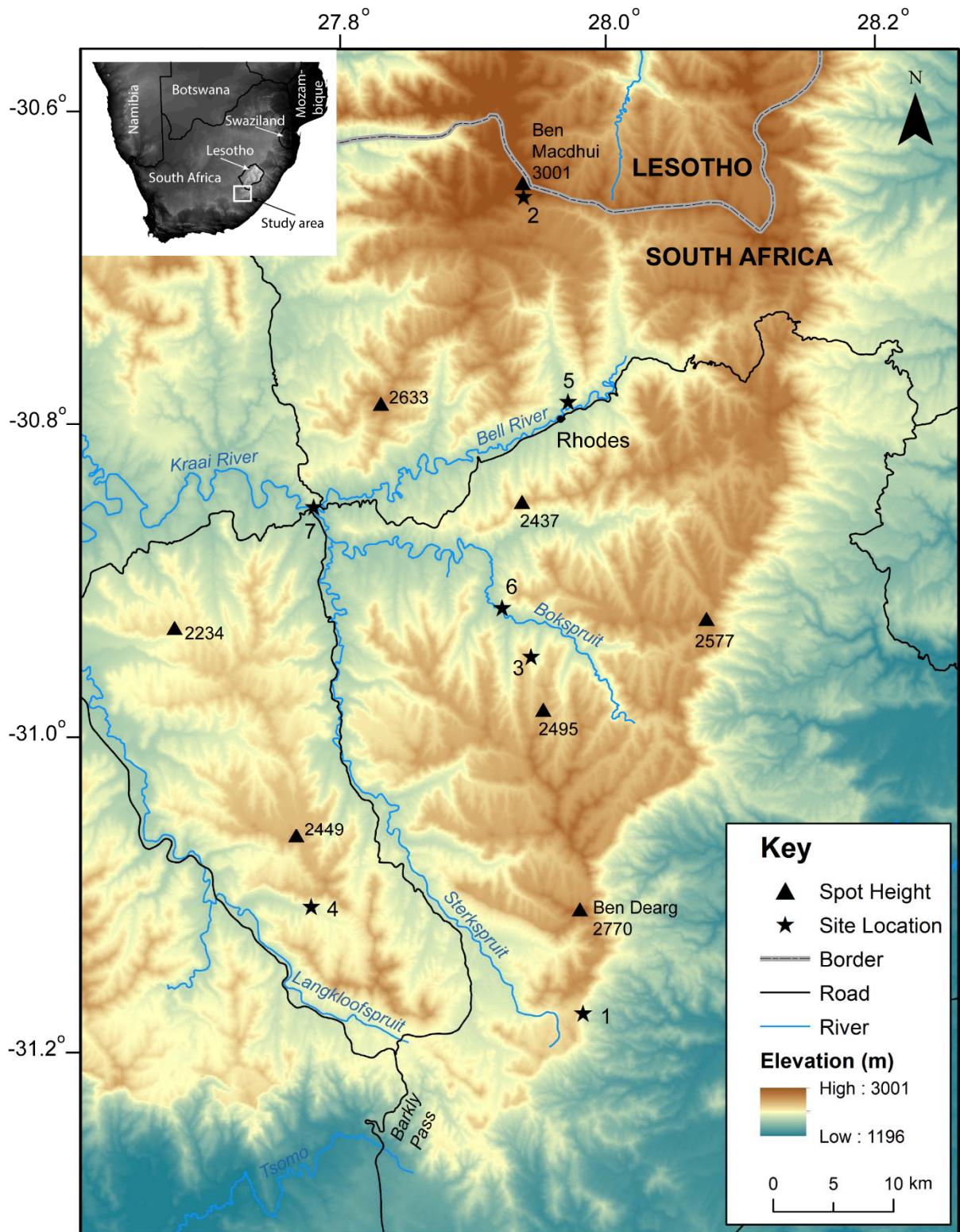


Figure 2

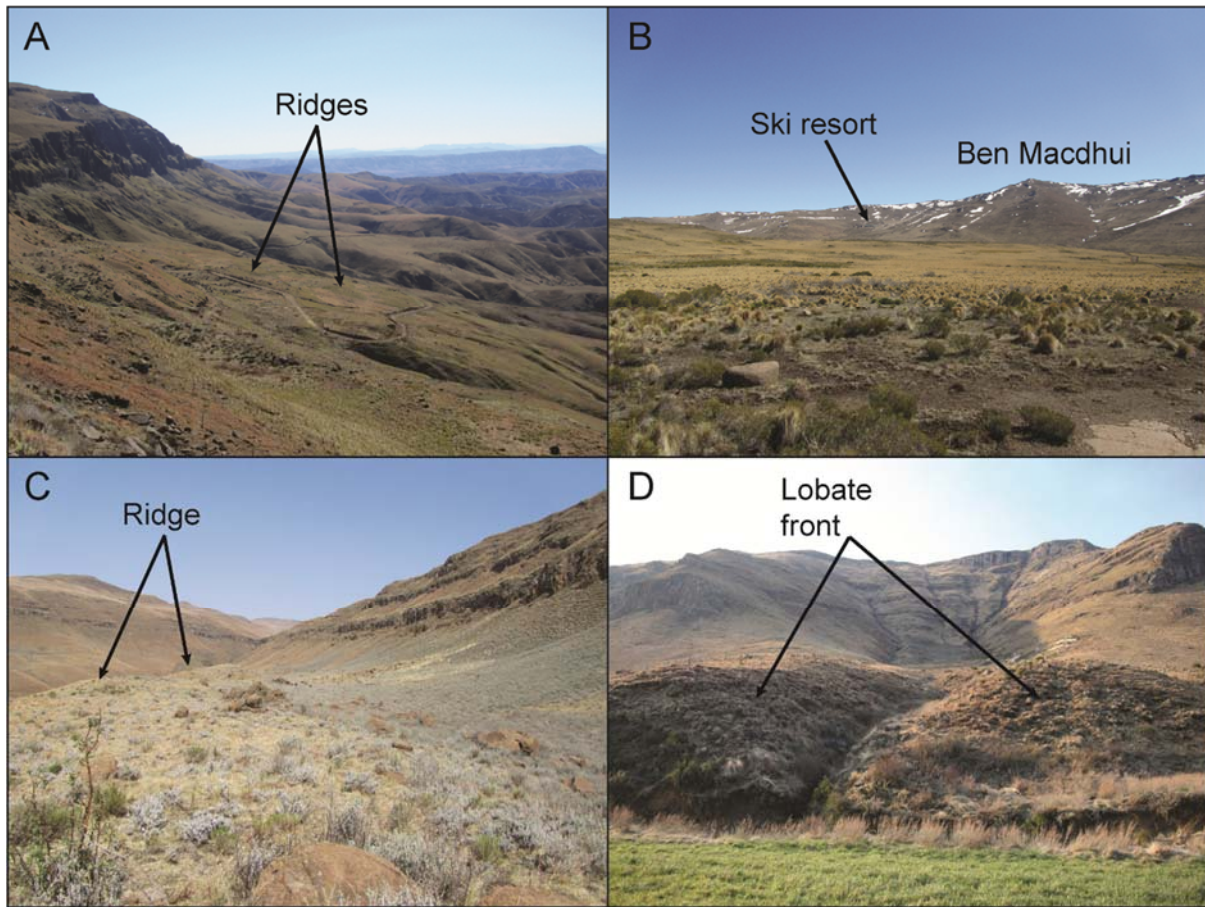


Figure 3

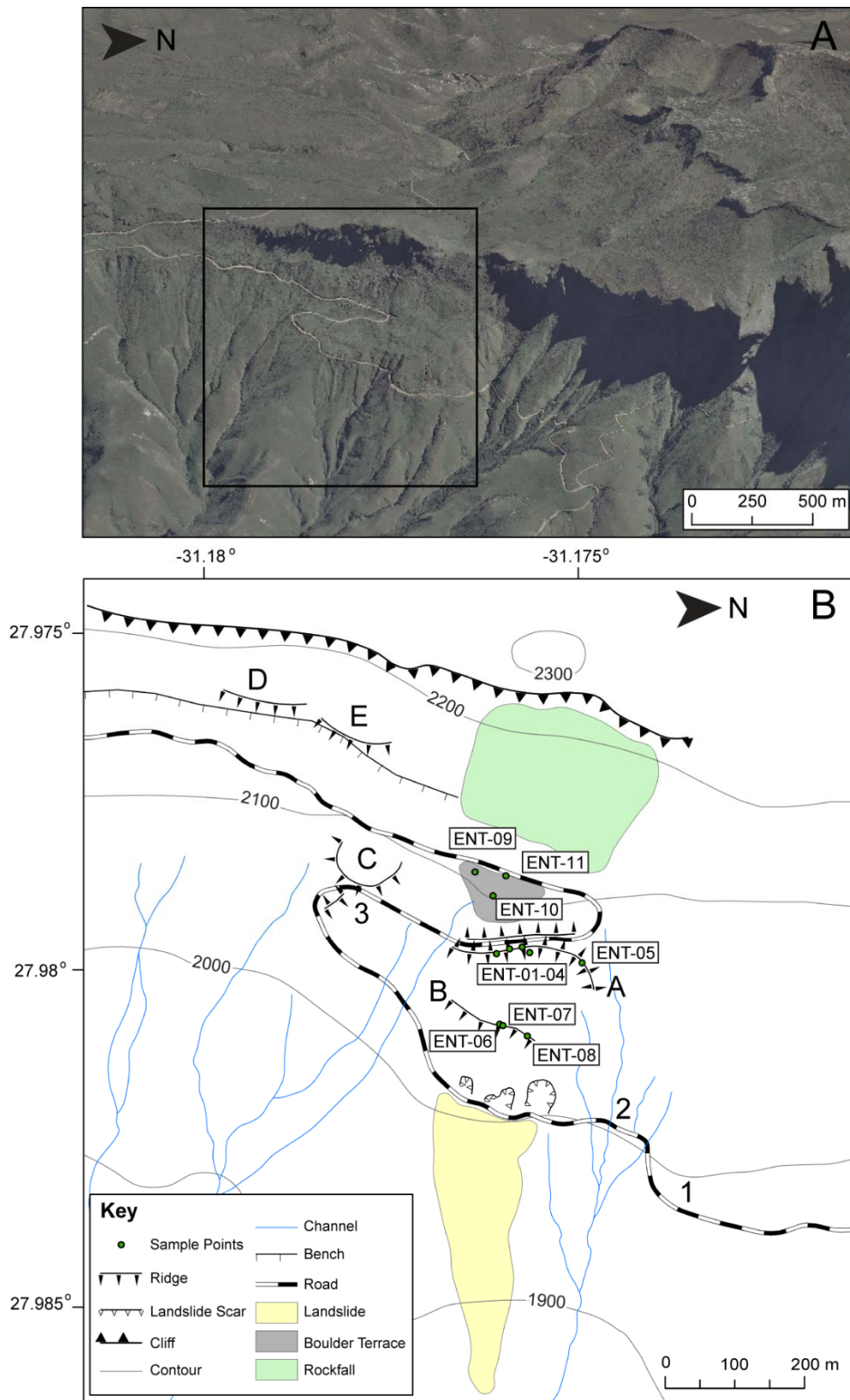


Figure 4

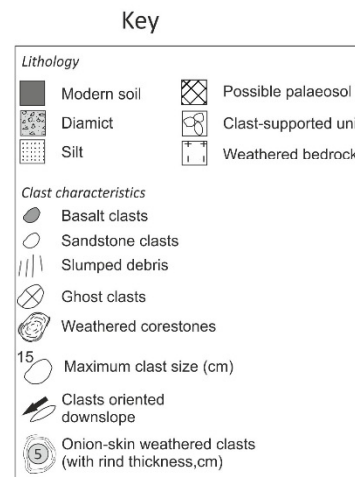
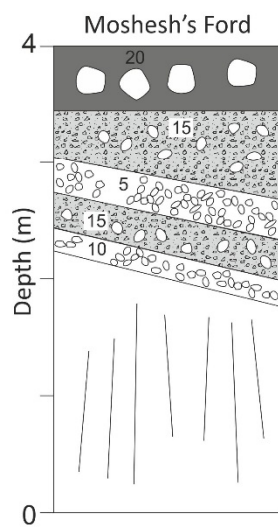
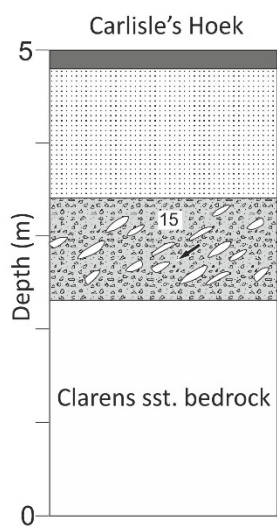
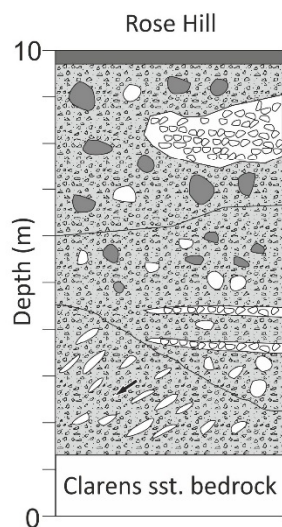
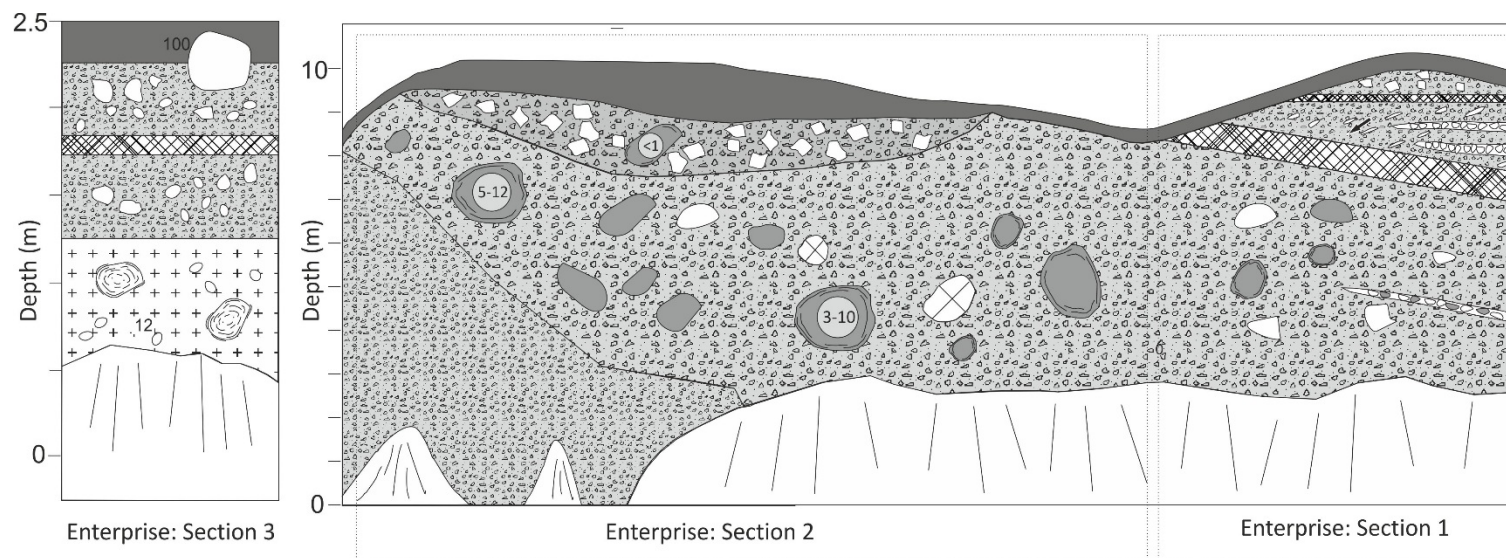


Figure 5



Figure 6

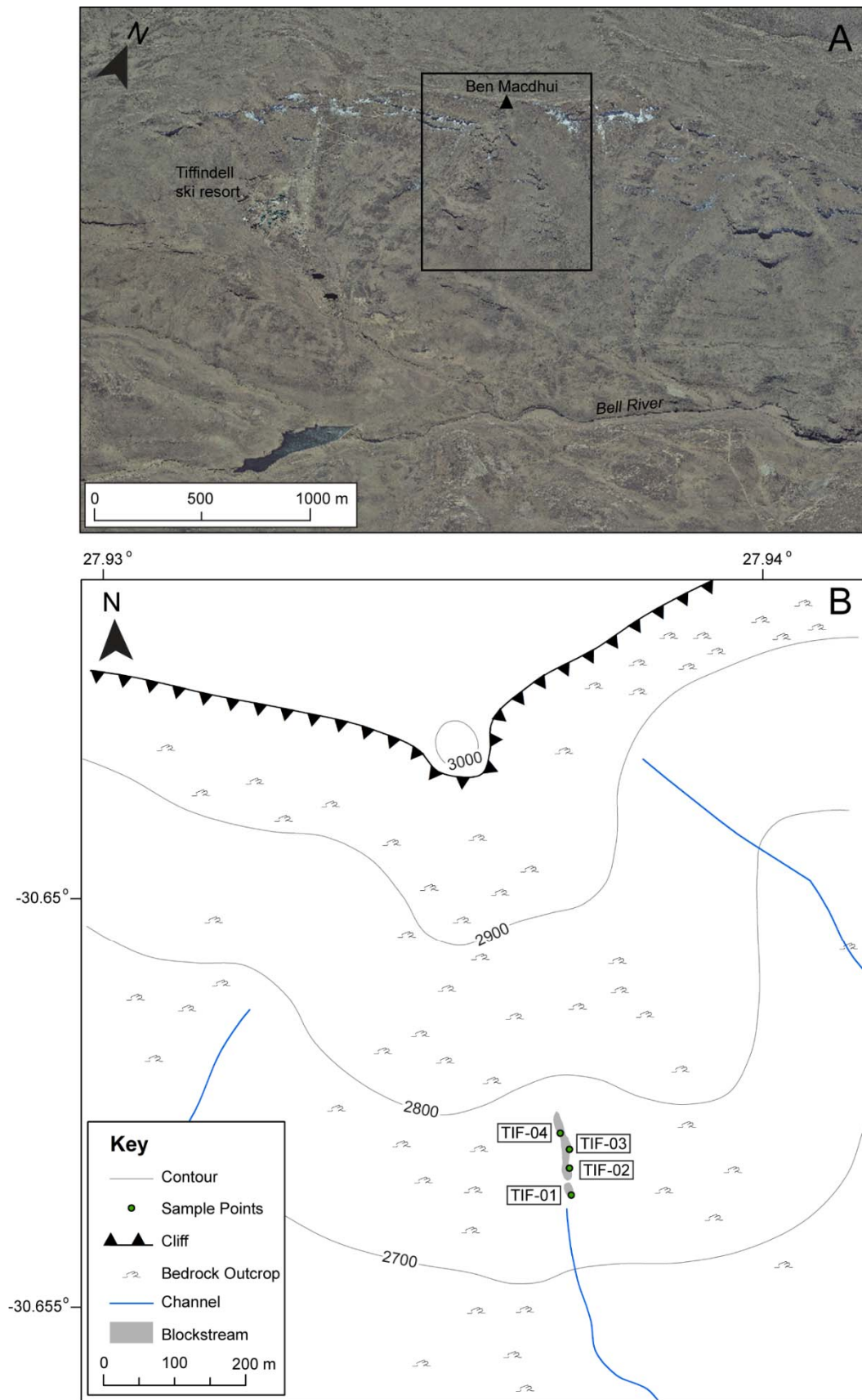


Figure 7

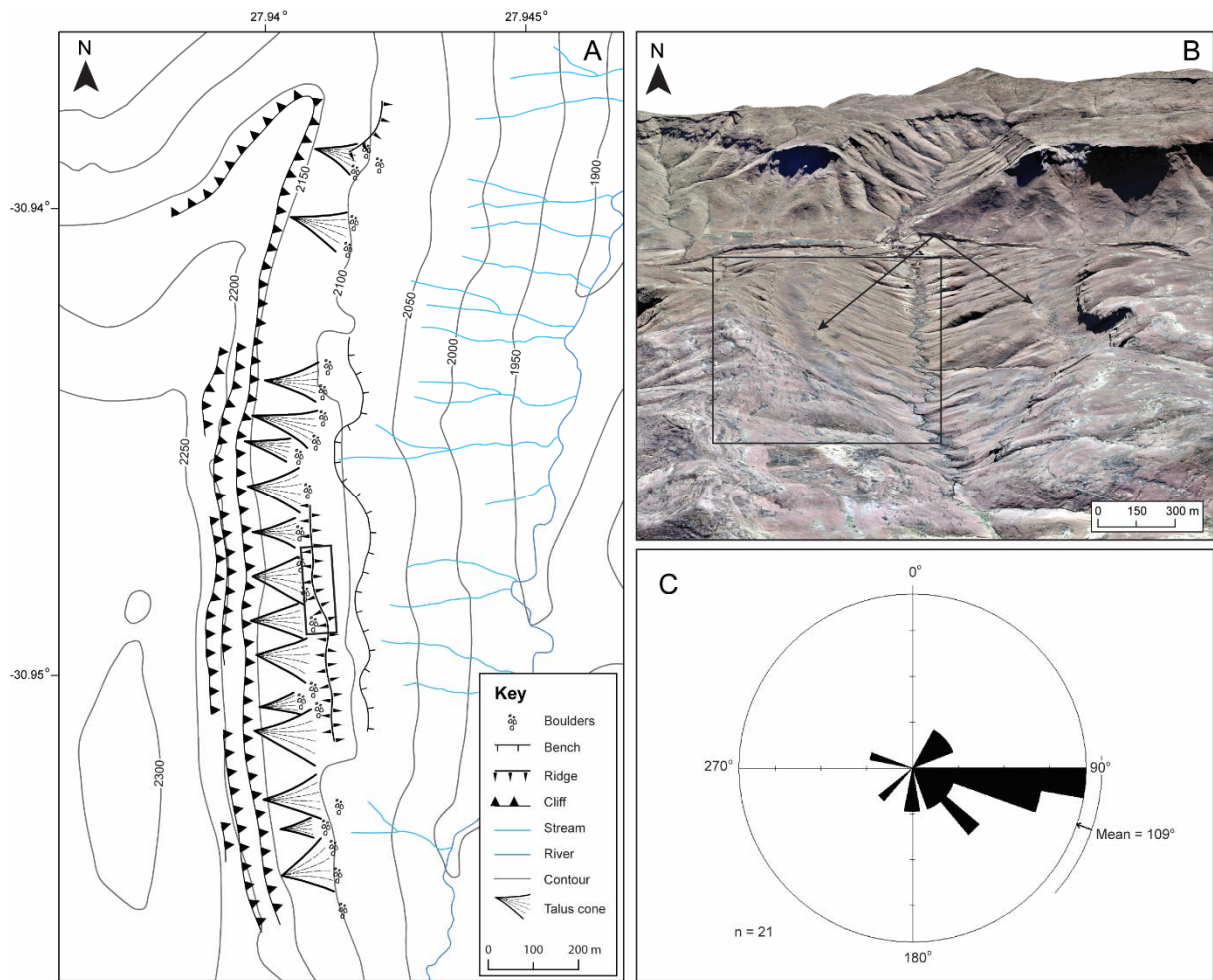


Figure 8



Figure 9

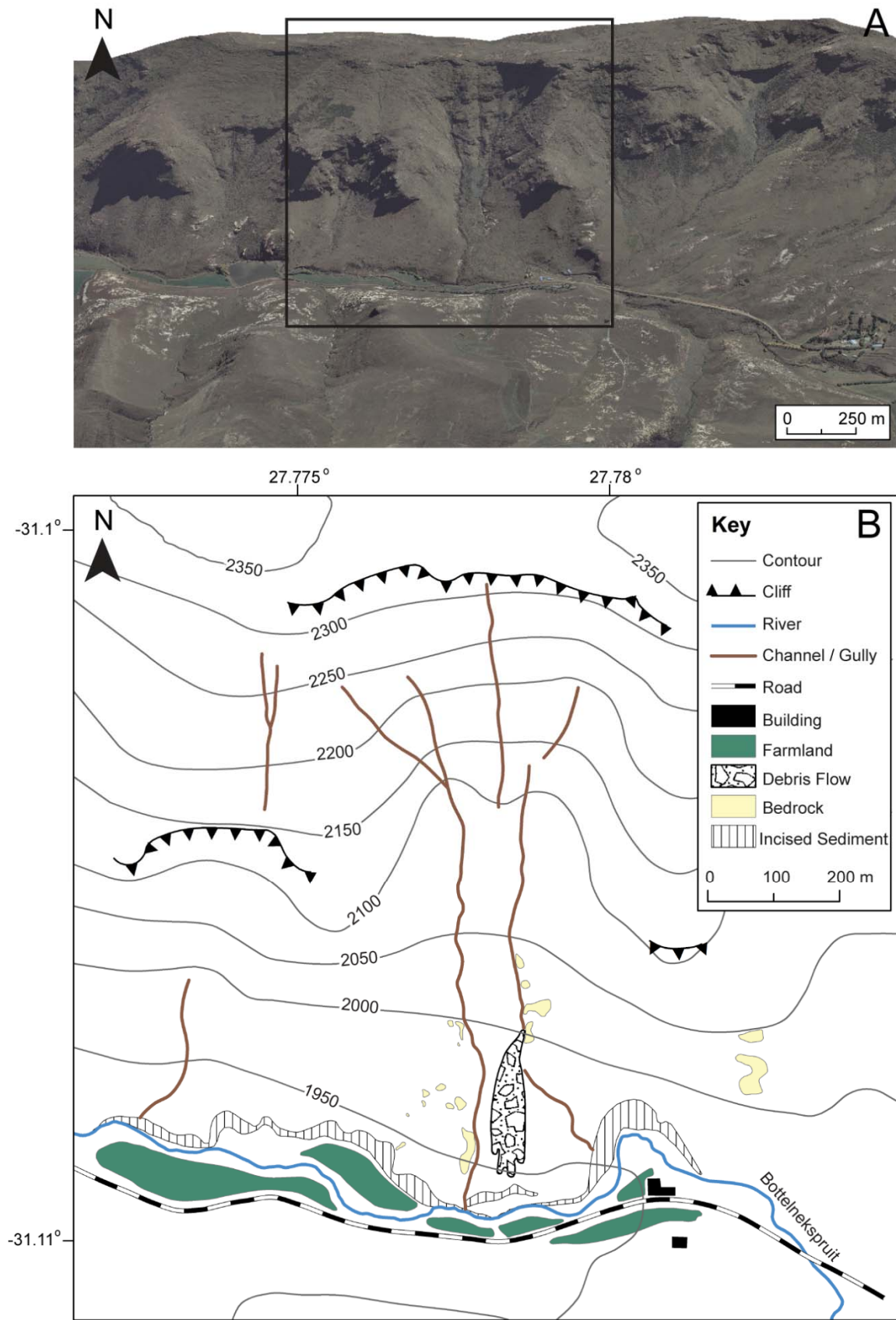


Table 1

Site information for the samples collected for surface exposure dating

Sample	Longitude (°E)	Latitude (°N)	Altitude (m) (GPS)	Altitude (m) (GIS)	Lithology ^a	Horizon correction	Thickness (cm) ^b
<i>Mount Enterprise</i>							
ENT-01	27.9798	31.1758	2087	2077	basalt	0.9864	1.8
ENT-02	27.9798	31.176	2084	2076	basalt	0.9864	2.8
ENT-03	27.9799	31.1761	2079	2068	basalt	0.9855	1.8
ENT-04	27.9799	31.1757	2073	2076	basalt	0.9854	2.9
ENT-05	27.98	31.175	2083	2075	basalt	0.9873	3.6
ENT-06	27.9809	31.1761	2052	2048	basalt	0.9902	2.4
ENT-07	27.981	31.176	2025	2048	basalt	0.9902	2.5
ENT-08	27.9811	31.1757	2044	2046	basalt	0.9905	2.0
ENT-09	27.98	31.18	2098	2100	basalt	0.9808	3.4
ENT-10	27.98	31.18	2105	2090	basalt	0.9808	4.1
ENT-11	27.98	31.18	2107	2098	basalt	0.9808	3.3
<i>Tiffindell</i>							
TIF-01	27.94	30.65	2712	2728	basalt	0.9871	2.3
TIF-02	27.94	30.65	2755	2754	basalt	0.9881	4.0
TIF-03	27.94	30.65	2772	2762	basalt	0.9854	2.6
TIF-04	27.94	30.65	2774	2775	basalt	0.9854	4.6

a. Basalt $\rho = 3.0 \text{ g.cm}^{-3}$.b. $L = 160 \text{ g.cm}^{-2}$.

Table 2³⁶Cl exposure ages for the sample sites^a

Sample	Lab code	[³⁶ Cl] _c (x10 ⁴ g ⁻¹) ^b	[³⁶ Cl] _r (x10 ² g ⁻¹) ^c	Exposure age (ka)
<i>Mount Enterprise</i>				
ENT-01	ANU-C248-21	18.65 ± 0.91	1.86 ± 0.14	10.3 ± 0.6
ENT-02	ANU-C248-22	23.83 ± 0.754	1.82 ± 0.75	9.8 ± 0.5
ENT-03	ANU-C248-23	23.57 ± 1.170	1.34 ± 0.11	12.0 ± 0.7
ENT-04	ANU-C249-09	16.94 ± 0.87	1.28 ± 0.12	9.2 ± 0.5
ENT-05	ANU-C248-24	20.04 ± 1.04	0.684 ± 0.099	11.3 ± 0.7
ENT-06	ANU-C248-25	26.79 ± 1.19	4.39 ± 0.28	11.2 ± 0.6
ENT-07	ANU-C248-26	38.02 ± 1.84	1.45 ± 0.28	20.5 ± 1.2
ENT-08	ANU-C248-27	32.56 ± 1.60	1.43 ± 0.12	17.5 ± 1.0
ENT-09	ANU-C248-28	14.29 ± 0.602	1.78 ± 0.099	7.6 ± 0.4
ENT-10	ANU-C248-29	14.93 ± 0.713	2.43 ± 0.15	7.7 ± 0.4
ENT-11	ANU-C249-11	9.332 ± 0.501	1.13 ± 0.11	5.0 ± 0.3
<i>Tiffindell</i>				
TIF-01	ANU-C249-06	127.7 ± 5.05	0.757 ± 0.064	49.3 ± 2.5
TIF-02	ANU-C249-03	39.45 ± 2.12	0.916 ± 0.063	13.6 ± 0.8
TIF-03	ANU-C249-04	77.99 ± 3.49	0.711 ± 0.060	26.1 ± 1.4
TIF-04	ANU-C249-05	38.88 ± 2.18	0.823 ± 0.056	12.7 ± 0.8

^aData are normalised to the GEC standard (³⁶Cl/Cl = 444 x 10⁻¹⁵).Carrier ³⁶Cl/Cl = 1 x 10⁻¹⁵.³⁶Cl decay constant 2.3 x 10⁻⁶ y⁻¹.

b. C = cosmogenic component.

c. R = background nucleogenic component.